# Utility of Aged Measurements for Localization

Wasif J. Hussain, Gaurav Duggal, Harpreet S. Dhillon, R. Michael Buehrer

Abstract-Many modern navigation scenarios involve autonomous agents navigating in an environment with a priori information of landmarks and obstacles. In such applications, agents make important navigation related decisions for avoiding obstacles. The agents often self-localize using Time-Of-Flight (TOF) measurements from known anchors by continuous sensorpolling. This polling uses system resources such as wireless spectrum and energy and a more opportunistic polling strategy would conserve these resources. For a previously obtained measurement, as the time elapses, the associated position information with this measurement ages. This is because the agent is continuously moving. Clearly, the nature of change of position information depends on the nature of the agent's motion. In this work, we investigate the time dependence of position information as previously obtained measurements age. We discuss two general motion models - linear and circular, associated with the agent's motion. Using the Cramer-Rao lower bound (CRLB), we analyze the effect of motion models and their influence on information content of aged sensor measurements. In particular for map based navigation systems, viewing an agent's trajectory as a combination of linear and circular motion between waypoints, we analyze the variation of position error bound (PEB) with age. Finally, we present our insights about opportunistic sensor polling to a mab based navigation scenario.

Index Terms-FIM, CRLB, PEB, AoI, Map based navigation

#### I. Introduction

Localization on a map is a fundamental challenge in navigation systems, crucial for ensuring accurate positioning, dynamic map updates and navigation. This process involves determining an agent's precise location within a given map. Due to the advancements in spectrum sharing and multiantenna diversity, radio based localization techniques have been garnering significant research interest of the community [1]–[3]. These techniques employ anchors with known positions to transmit reference signals to the agent which is to be localized. Based on wireless signal measurements like time of flight, angle of arrival/departure, signal strength, etc, there exists a number of techniques for estimating the agent's position [4].

For localization in an adversarial environment, communication channels can often be jammed [5] or experience long propagation delays [6], [7] before the information can be processed to obtain location estimates. Further non-cooperative agents try to minimize their transmissions in order to avoid getting detected [8]. In such scenarios, there is a need to investigate the information content about the current location in aged measurements combined with a motion model. Insights about the decay of information with time can be used to prevent unnecessary transmissions thereby preserving secrecy.

The authors are with Wireless@VT, Virginia Tech, Blacksburg, VA 24061 USA (e-mail: wasif, gduggal, hdhillon, rbuehrer@vt.edu). The support of US NSF (grants CNS-1923807 and CNS-2107276) is gratefully acknowledged.

The motion model captures the time evolution of the agent's position and we study the impact two general motion models have on the information decay. The past location is derived from measurements which are obtained by polling different sensors.

With each poll there is an associated uncertainty in the position estimate which propagates with time according to the motion model. The motion models we consider are defined by a point with a known position, termed as a waypoint, and a function that describes the agent's movement.

Waypoints are commonly used in map based navigation systems. For example, in [9], the authors identified waypoints as a means to produce a map which can be used to aid the robot in navigating the environment. In [10], the authors developed optimization framework for path planning navigation system by solving a multi-objective shortest path problem which gives optimum routes using information about stored waypoints in a database. In [11], a simultaneous localization and mapping (SLAM) algorithm based on K-means clustering utilizing self-detected waypoints is introduced to localize a robot in its environment. In [12], the authors modelled turning movement of vehicles on roads as circular arcs with known origin.

Note, Kalman filters have been widely used to study navigation problems because of their ability to combine polled sensor data with motion model predictions [13], [14]. While Kalman filters require polling of new measurements to merge them with the location estimate from the previous state, there arises a very interesting question here. Do the old measurements along with the motion model alone suffice to yield meaningful position accuracy? Answering this question rigorously could provide important insights into optimal resource allocation and the value of stale information in positioning and navigation problems.

Age of information (AoI) has been studied as an important performance metric to quantify the freshness of information by the time it reaches the processing nodes for various cyber-physical applications. These applications require status updates to be as fresh as possible but this comes with a tradeoff with system resources and processing capabilities or in adversarial scenarios may not even be possible. In [15], the authors described the latest design and optimization approaches for cyber-physical systems from an AoI perspective. In [16], the authors presented a joint stochastic geometry based analysis of throughput and AoI performance metrics in a cellular IoT network and characterised the spatial variation in AoI performance of status update links. In [17], the authors derived closed form expressions to characterise coverage in a cyber-physical system monitoring an environmental variable modeled as a spatio-temporal process.

To the best of our knowledge the value and role of age in range measurements of a localization system has not been studied before. Informed by this major gap, we make the following contributions in this paper.

- Age of information in Positioning: We explore the role of AoI in localization problems by developing a mathematical framework that captures the staleness in positioning measurements using a time dependent CRLB formulation.
- Role of motion models: We show that motion models play a significant role in determining the utility of aged range measurements. Our work analyzes two general motion models applicable to various scenarios and in particular to map based navigation systems.
- System design insights: We perform numerical simulations for a map based localization system and offer insights on optimal frequency of polling and waypoint placement.

#### II. SYSTEM MODEL AND PRELIMINARIES

We analyze two types of motion models, namely, linear (guided) and circular. These two motion models have been rigorously employed and studied in literature for a multitude of research problems involving mobile agents [9], [10], [12]. Using our framework we can analyze more general trajectories by discretizing them piecewise into guided linear motions and circular turns.

We want to study the importance of initial range measurements for the estimation of future positions  $(x_n, y_n)$  which are a function of initial position  $(x_o, y_o)$  and age  $(\delta)$  according to a deterministic motion model, in general described as:

$$x_n = g_1(x_o, y_o, \delta)$$
  

$$y_n = g_2(x_o, y_o, \delta)$$
(1)

where  $g_1(.), g_2(.)$  are functions modeling the true trajectory of the agent. Therefore any uncertainty in the estimation of  $(x_o, y_o)$  contributes to an uncertainty in estimation future positions (using the same set of measurements) as implied by the above equation.

## A. Linear motion model

This model captures an agent's motion towards a known waypoint as illustrated in Fig. 1. The agent moves in a straight line directed towards the respective waypoint $(x_t, y_t)$  with a constant speed v. Initially the agent has no information about its position and direction of motion, which it estimates through range measurements. The current position  $(x_o, y_o)$  is related to its orientation  $(\theta)$  with respect to the waypoint as follows:

$$\tan(\theta) = \frac{y_t - y_o}{x_t - x_o}. (2)$$

Thus the future position  $(\mathbf{p_{new}} = (x_n, y_n))$  after a time  $\delta$  can be written as:

$$x_n = x_o + v\delta\cos(\theta)$$
  

$$y_n = y_o + v\delta\sin(\theta)$$
 (3)

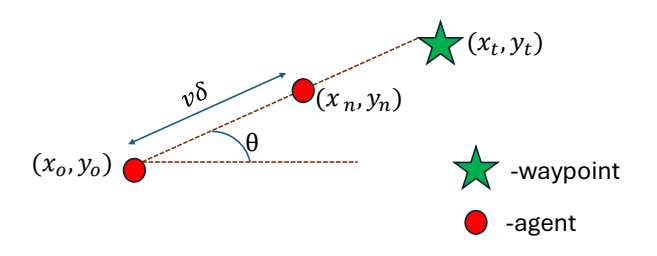


Fig. 1. Illustration of the linear motion model.

#### B. Circular motion model

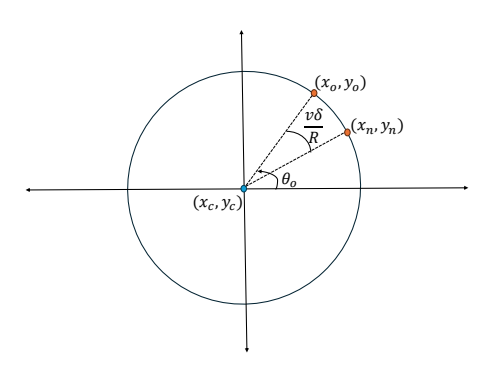


Fig. 2. Illustration of the circular motion model.

This model is used for capturing the turning motion of an agent as illustrated in Fig. 2. The agent moves in a circular trajectory around a known waypoint  $(x_c, y_c)$  with a fixed radius  $R_c = \sqrt{(x_o - x_c)^2 + (y_o - y_c)^2}$  as determined by its initial position, having a constant linear velocity v in anticlockwise (without loss of generality) direction. The agent has no information about its position, turning radius or initial orientation  $\left(\theta_o = \tan^{-1}\left(\frac{y_o - y_c}{x_o - x_c}\right)\right)$  with respect to x-axis. The relation between current position and position after a

time  $\delta$  is given as:

$$x_n = x_c + R_c \cos\left(\theta_o - \frac{v\delta}{R_c}\right)$$

$$y_n = y_c + R_c \sin\left(\theta_o - \frac{v\delta}{R_c}\right)$$
(4)

# C. CRLB analysis

CRLB provides a lower bound on the variance of any unbiased estimator  $(\hat{\Theta}(\bar{y}))$  of a parameter  $\Theta = (\theta_1, \dots, \theta_n)$ from a sample of observations of a random variable  $\bar{y}$  with pdf given by  $f(\bar{y}; \Theta)$ . Mathematically it is defined as:

$$CRLB(\mathbf{\Theta}) = \mathbb{E}_{\mathbf{\Theta}} \left\{ \left( \hat{\mathbf{\Theta}} - \mathbf{\Theta} \right) \left( \hat{\mathbf{\Theta}} - \mathbf{\Theta} \right)^T \right\} \ge \mathbf{I}_{\mathbf{\Theta}}^{-1}.$$
 (5)

where

$$\mathbf{I}_{\boldsymbol{\Theta}} = \mathbb{E}_{\boldsymbol{\Theta}} \left\{ \left( \frac{\partial \log f(\bar{\mathbf{y}}; \boldsymbol{\Theta})}{\partial \boldsymbol{\Theta}} \right) \left( \frac{\partial \log f(\bar{\mathbf{y}}; \boldsymbol{\Theta})}{\partial \boldsymbol{\Theta}} \right)^T \right\}. \quad (6)$$

is called the Fisher information matrix (FIM). It quantifies the amount of information contained in observations of a random variable about a parameter which influences the probability distribution of this random variable. For matrices  $\bf A$  and  $\bf B$ ,  $\bf A \geq \bf B$  implies that  $\bf A - \bf B$  is a positive semi-definite matrix.

When  $\Theta$  is a position parameter, *i.e*  $\Theta=(x,y,z)$ , then the position error bound (PEB) for the estimation of  $\Theta$  is calculated as:

$$PEB = \sqrt{Trace(CRLB(\mathbf{\Theta}))}.$$
 (7)

When estimating a function of the parameter  $\Theta$  defined as  $\alpha = \mathbf{g}(\Theta) = (g_1(\theta_1), \dots, g_m(\theta_n))$ , the CRLB is transformed as [18]:

$$CRLB(\alpha) = \mathbf{J}_{\Theta \to \alpha} \mathbf{I}_{\Theta}^{-1} \mathbf{J}_{\Theta \to \alpha}^{T}.$$
 (8)

where  $J_{\Theta \to \alpha}$  is the Jacobian matrix defined as [18]:

$$\mathbf{J}_{\boldsymbol{\Theta} \to \boldsymbol{\alpha}} = \frac{\partial \mathbf{g}(\boldsymbol{\Theta})}{\partial \boldsymbol{\Theta}} = \begin{bmatrix} \frac{\partial g_1(\boldsymbol{\Theta})}{\partial \theta_1} & \frac{\partial g_1(\boldsymbol{\Theta})}{\partial \theta_2} & \dots & \frac{\partial g_1(\boldsymbol{\Theta})}{\partial \theta_n} \\ \vdots & \vdots & \ddots & \vdots \\ \frac{\partial g_m(\boldsymbol{\Theta})}{\partial \theta_1} & \frac{\partial g_m(\boldsymbol{\Theta})}{\partial \theta_2} & \dots & \frac{\partial g_m(\boldsymbol{\Theta})}{\partial \theta_n} \end{bmatrix}.$$

### III. MAP BASED NAVIGATION

In this section we will apply the framework introduced in Section II to a map-based navigation scenario where an agent has to navigate in an environment following a trajectory defined in terms of waypoints and turn around respective obstacle corners as illustrated in Fig. 3. The map has perfect knowledge of the waypoint locations and the obstacle corners. In such applications the agents commonly use camera cues for identifying waypoints [19], [20]. We assume that the agent is able to align itself with negligible error in the direction of waypoint relative to its frame. Once it has aligned itself, it starts to move towards the waypoint at a constant speed. We define polling as the agent obtaining range measurements and the environment's visuals. The turning movements can be approximated as circular arcs around respective obstacle corners. Our objective is to determine the agent's position during the course of following this trajectory, minimizing the frequency of polling.

For numerical simulation we used time of flight (TOF) based localization, however our analysis can be easily extended to other methods like AOA, TDOA, etc as well.

For obtaining the TOF measurements we use a total of B anchors whose positions  $\{(x_i,y_i),H_i\}_{i=1}^B$  are perfectly known

The received signal at the agent from the j-th anchor is given as:

$$y_j(t) = \alpha_j s(t - \tau_j) + v_j \quad \forall j \in \{1, \dots, B\}.$$
 (10)

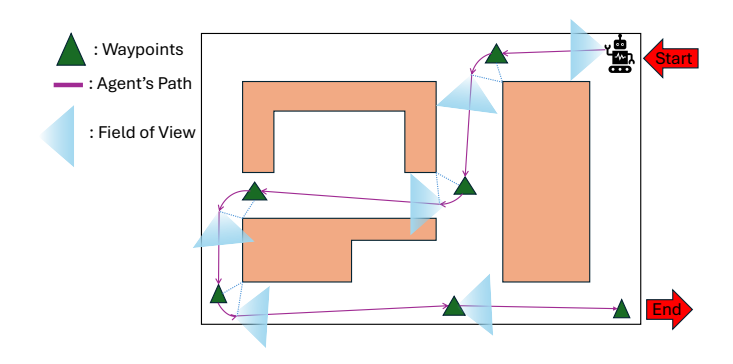


Fig. 3. Illustration of the map-based navigation scenario.

where s(t) is the known reference signal waveform transmitted by the anchors,  $\tau_j$  is the time of arrival or the propagation delay between the j-th anchor and the agent,  $\alpha_j$  is the gain for the channel between j-th anchor and the agent, and  $v_j$  is additive white Gaussian noise (AWGN). These TOF measurements can be used for estimating the position of agents using a number of techniques [4].

We will now derive the CRLB for the estimation of current agent location  $(x_n, y_n)$  based on aged range measurements.

### A. FIM derivation

The FIM for estimating propagation delay from each anchor in a TOF system is given as [18]:  $I_{\tau} = \Omega^{-1}$ , where,

$$\mathbf{\Omega} = \begin{bmatrix} \omega_1^2 & 0 & \dots & 0 \\ 0 & \omega_2^2 & \dots & 0 \\ \vdots & \vdots & \ddots & \vdots \\ 0 & 0 & \dots & \omega_B^2 \end{bmatrix}; \omega_i = \frac{1}{8\pi^2 \eta^2 \text{SNR}_i}. \tag{11}$$

where  $\eta = \sqrt{\frac{\int f^2 |S(f)|^2 df}{\int |S(f)|^2 df}}$  is the normalized bandwidth, S(f) denotes the Fourier transform of the reference transmit signal s(t) and  $\mathrm{SNR}_i$  is the signal to noise ratio between i-th anchor and the agent.

Let 
$$\Theta_o = \{\underbrace{x_o, y_o}, \Delta_1, \dots, \Delta_B\}$$
 denote the position param-

eter. Here,  $\Delta_i$  is the NLOS bias parameter between the *i*-th anchor and the agent which captures the signal distortion due to obstacles blocking the direct path between the transmitter and the receiver, a common occurrence in agent navigation problems. The following inverse transformation is used for modeling the Jacobian  $\mathbf{J}_{\tau\to\Theta_0}$ 

$$\tau_{i} = \frac{\sqrt{(x_{o} - x_{i})^{2} + (y_{o} - y_{i})^{2} + H_{i}^{2}} + \Delta_{i}}{c} 
\frac{\partial \tau_{i}}{\partial x_{o}} = \frac{(x_{o} - x_{i})}{\sqrt{(x_{o} - x_{i})^{2} + (y_{o} - y_{i})^{2} + H_{i}^{2}}} 
\frac{\partial \tau_{i}}{\partial y_{o}} = \frac{(y_{o} - y_{i})}{\sqrt{(x_{o} - x_{i})^{2} + (y_{o} - y_{i})^{2} + H_{i}^{2}}} 
\frac{\partial \tau_{i}}{\partial \Delta_{j}} = \begin{cases} \frac{1}{c}, & i = j \\ 0, & i \neq j \end{cases}$$
(12)

The Jacobian for transformation is given as:

$$\mathbf{J}_{\tau \to \Theta_o} = \begin{bmatrix} \frac{\partial \tau_1}{x_o} & \frac{\partial \tau_2}{x_o} & \dots & \frac{\partial \tau_B}{x_o} \\ \frac{\partial \tau_1}{\partial \tau_1} & \frac{\partial \tau_2}{\partial y_o} & \dots & \frac{\partial \tau_B}{\partial y_o} \\ \frac{\partial \tau_1}{\partial \Delta_1} & \frac{\partial \tau_2}{\partial \Delta_1} & \dots & \frac{\partial \tau_B}{\partial \Delta_1} \\ \vdots & \vdots & \ddots & \vdots \\ \frac{\partial \tau_1}{\partial \Delta_B} & \frac{\partial \tau_2}{\partial \Delta_B} & \dots & \frac{\partial \tau_B}{\partial \Delta_B} \end{bmatrix} . \tag{13}$$

Accordingly FIM for  $\Theta_0$  can be calculated as:

$$\mathbf{I}_{\mathbf{\Theta}_{\mathbf{O}}} = \mathbf{J}_{\tau \to \mathbf{\Theta}_{\mathbf{O}}} \mathbf{I}_{\tau} \mathbf{J}_{\tau \to \mathbf{\Theta}_{\mathbf{O}}}^{T}. \tag{14}$$

Prior information about the parameters can be incorporated to get the resultant generalized FIM [1] as:

$$\mathbf{I}_{o} = \mathbf{I}_{\mathbf{\Theta}_{o}} + \mathbf{I}_{P_{o}},\tag{15}$$

where  $I_{P_o}$  is the prior information about  $\Theta_o$  which can be calculated using the prior probability density functions as follows:

$$f(\mathbf{\Theta}_{o}) = f(\mathbf{p}_{old}) \prod_{j=1}^{B} f(\Delta_{j})$$

$$\mathbf{I}_{P_{o}} = \mathbf{E}_{\mathbf{\Theta}_{o}} \left\{ \left( \frac{\partial \log f(\mathbf{\Theta}_{o})}{\partial \mathbf{\Theta}_{o}} \right) \left( \frac{\partial \log f(\mathbf{\Theta}_{o})}{\partial \mathbf{\Theta}_{o}} \right)^{T} \right\}.$$
(16)

We have assumed the position and bias parameters to be independent. The NLOS bias  $\Delta_j$  is assumed to be Gamma distributed with shape parameter  $k_a$  and variance  $\sigma_{\Delta}^2$  [3]. Using these we can obtain  $\mathbf{I}_{P_o}$  as:

$$\mathbf{I}_{\mathbf{P}_{o}} = \begin{bmatrix} \mathbf{0}_{2\times2} & \mathbf{0}_{2\times B} \\ \mathbf{0}_{B\times2} & \frac{k_{a}}{k_{a}-2} \frac{1}{\sigma_{\Delta}^{2}} \mathbf{I}_{B\times B} \end{bmatrix}. \tag{17}$$

To obtain the CRLB we need to invert the generalized FIM which is a high dimension matrix. Since we are only interested in a subset of parameters  $\mathbf{p}_{\text{old}}$ , we can formulate an effective FIM (EFIM) [1] denoted as  $\mathbf{I}_{\mathbf{p}_{\text{old}}} = \mathbf{A} - \mathbf{D}\mathbf{C}^{-1}\mathbf{D}^T$ . The CRLB can be obtained as  $\mathbf{I}_{\mathbf{p}_{\text{old}}}^{-1}$ . Where  $\mathbf{A}, \mathbf{C}, \mathbf{D}$  are obtained from the structure of the generalized FIM in (15) given as:

$$\mathbf{I}_{o} = \begin{bmatrix} \mathbf{A}_{2\times2} & \mathbf{D}_{2\times B} \\ \mathbf{D}_{R\times2}^{T} & \mathbf{C}_{B\times B} \end{bmatrix}.$$
 (18)

## B. Transformation Jacobians

1) Linear motion model: The entries of Jacobian matrix for transforming old positions to new positions are given as:

$$R_{o} = \sqrt{(y_{t} - y_{o})^{2} + (x_{t} - x_{o})^{2}}$$

$$\frac{\partial x_{n}}{\partial x_{o}} = 1 - \frac{v\delta}{R_{o}} \sin^{2}(\theta), \quad \frac{\partial x_{n}}{\partial y_{o}} = \frac{v\delta}{R_{o}} \sin(\theta) \cos(\theta)$$

$$\frac{\partial y_{n}}{\partial x_{o}} = \frac{v\delta}{R_{o}} \sin(\theta) \cos(\theta), \quad \frac{\partial y_{n}}{\partial y_{o}} = 1 - \frac{v\delta}{R_{o}} \cos^{2}(\theta). \quad (19)$$

$$\mathbf{J}_{\mathbf{p}_{\text{old}} \to \mathbf{p}_{\text{new}}} = \begin{bmatrix} \frac{\partial x_{n}}{\partial y_{o}} & \frac{\partial x_{n}}{\partial y_{o}} \\ \frac{\partial y_{n}}{\partial x_{o}} & \frac{\partial y_{n}}{\partial y_{o}} \end{bmatrix}$$

2) Circular motion model: The entries of Jacobian matrix for transforming old positions to new positions are given as:

$$\frac{\partial \theta_{o}}{\partial x_{o}} = \frac{-\sin(\theta_{o})}{R_{c}}, \quad \frac{\partial \theta_{o}}{\partial y_{o}} = \frac{\cos(\theta_{o})}{R_{c}}$$

$$\frac{\partial R_{c}}{\partial x_{o}} = \frac{x_{o} - x_{c}}{R_{c}}, \quad \frac{\partial R_{c}}{\partial y_{o}} = \frac{y_{o} - y_{c}}{R_{c}}$$

$$\frac{\partial x_{n}}{\partial x_{o}} = \cos\left(\theta_{o} - \frac{v\delta}{R_{c}}\right) \frac{\partial R_{c}}{\partial x_{o}} - R_{c} \sin\left(\theta_{o} - \frac{v\delta}{R_{c}}\right) \left(\frac{\partial \theta_{o}}{\partial x_{o}} + \frac{v\delta}{R_{c}^{2}} \frac{\partial R_{c}}{\partial x_{o}}\right)$$

$$\frac{\partial x_{n}}{\partial y_{o}} = \cos\left(\theta_{o} - \frac{v\delta}{R_{c}}\right) \frac{\partial R_{c}}{\partial y_{o}} - R_{c} \sin\left(\theta_{o} - \frac{v\delta}{R_{c}}\right) \left(\frac{\partial \theta_{o}}{\partial y_{o}} + \frac{v\delta}{R_{c}^{2}} \frac{\partial R_{c}}{\partial y_{o}}\right)$$

$$\frac{\partial y_{n}}{\partial x_{o}} = \sin\left(\theta_{o} - \frac{v\delta}{R_{c}}\right) \frac{\partial R_{c}}{\partial x_{o}} + R_{c} \cos\left(\theta_{o} - \frac{v\delta}{R_{c}}\right) \left(\frac{\partial \theta_{o}}{\partial x_{o}} + \frac{v\delta}{R_{c}^{2}} \frac{\partial R_{c}}{\partial x_{o}}\right)$$

$$\frac{\partial y_{n}}{\partial y_{o}} = \sin\left(\theta_{o} - \frac{v\delta}{R_{c}}\right) \frac{\partial R_{c}}{\partial x_{o}} + R_{c} \cos\left(\theta_{o} - \frac{v\delta}{R_{c}}\right) \left(\frac{\partial \theta_{o}}{\partial y_{o}} + \frac{v\delta}{R_{c}^{2}} \frac{\partial R_{c}}{\partial x_{o}}\right)$$

$$\frac{\partial y_{n}}{\partial y_{o}} = \sin\left(\theta_{o} - \frac{v\delta}{R_{c}}\right) \frac{\partial R_{c}}{\partial y_{o}} + R_{c} \cos\left(\theta_{o} - \frac{v\delta}{R_{c}}\right) \left(\frac{\partial \theta_{o}}{\partial y_{o}} + \frac{v\delta}{R_{c}^{2}} \frac{\partial R_{c}}{\partial y_{o}}\right)$$

$$\mathbf{J}_{\mathbf{p}_{old} \to \mathbf{p}_{new}} = \begin{bmatrix} \frac{\partial x_{n}}{\partial x_{o}} & \frac{\partial x_{n}}{\partial y_{o}} \\ \frac{\partial y_{n}}{\partial x_{o}} & \frac{\partial y_{n}}{\partial y_{o}} \end{bmatrix}$$
(20)

Using (8) we can write:

$$CRLB(\mathbf{p}_{new}) = \mathbf{J}_{\mathbf{p}_{old} \to \mathbf{p}_{new}} \mathbf{I}_{\mathbf{p}_{old}}^{-1} \mathbf{J}_{\mathbf{p}_{old} \to \mathbf{p}_{new}}^{T}.$$
 (21)

We now establish the following theorem to investigate the effect on PEB produced by a Jacobian matrix transformation.

Theorem 1 (Owstrowski): Let  $A \in \mathbb{R}^{n \times n}$  be a symmetric matrix and let  $X \in \mathbb{R}^{n \times n}$ . Denote  $\lambda_i(M)$  as the *i*-th eigen value of M in increasing order,  $1 \le i \le n$ . Then [21]:

$$\lambda_i(X^T A X) = \beta_i \lambda_i(A), \quad i = 1:n, \tag{22}$$

where  $\lambda_1(X^TX) \leq \beta_i \leq \lambda_n(X^TX)$ .

Corollary 1: The PEB for estimation of new position from aged measurements is bounded with respect to initial PEB as:

$$\sigma_1^2 \text{PEB(old)} \le \text{PEB(new)} \le \sigma_n^2 \text{PEB(old)},$$
 (23)

where  $\sigma_1$  and  $\sigma_n$  are the smallest and largest singular value of the transformation Jacobian  $\mathbf{J}_{\mathbf{p}_{\mathrm{old}} \to \mathbf{p}_{\mathrm{new}}}$  respectively. This can be shown by noting that trace of a matrix is the sum of its eigen values.

# IV. NUMERICAL RESULTS AND DISCUSSIONS

In this section we present numerical results from CRLB analysis and discuss key insights.

For simulation we chose 4 anchors which were placed at the vertex of a square of length  $100\mathrm{m}$  centered at the origin and at a height of  $10\mathrm{m}$ . We ensured that the agent's trajectory lies sufficiently inside the square to avoid anchor geometry effects [4]. We assumed constant SNR level of  $10\mathrm{dB}$  for the link between anchors and the agent. Bandwidth was taken as  $20~\&30~\mathrm{MHz}$ . The shape parameter for NLOS bias was taken as  $k_a=4$  and the mean was taken as  $2\mathrm{m}$ .

In Fig. 4, we compare the PEB of the future positions based on aged range measurements versus the PEB achieved by taking new measurements at that instant for the linear motion model. Contrary to the expectation that age always decays information content, we observe that using aged range measurement gives us better performance then taking a fresh measurements at that instant. This can be intuitively explained

because we are combining additional information that the agent moves towards a specific location (the waypoint) with the already available position information.

Let  $\delta_o = \frac{R_o}{v}$  denote the time required by the agent to reach the waypoint. Define  $\kappa = \frac{\delta}{\delta_o}$ . Upon simplifying  $\mathbf{J}_{\mathbf{p}_{\mathrm{old}} \to \mathbf{p}_{\mathrm{new}}}$  for the Jacobian in (19), we get:

$$\mathbf{J}_{\mathbf{p}_{\text{old}} \to \mathbf{p}_{\text{new}}} \mathbf{J}_{\mathbf{p}_{\text{old}} \to \mathbf{p}_{\text{new}}}^{T} = \begin{bmatrix} 1 & 0 \\ 0 & 1 \end{bmatrix} + (\kappa^{2} - 2\kappa) \begin{bmatrix} \sin^{2}(\theta) & -\sin(\theta)\cos(\theta) \\ -\sin(\theta)\cos(\theta) & \cos^{2}(\theta) \end{bmatrix}.$$
(24)

The singular values obtained are:  $\sigma_1^2 = 1$  and  $\sigma_2^2 = 1 + \kappa(\kappa - 2)$ .

We observe that the  $\max(\sigma_1^2, \sigma_2^2) = 1$  for  $0 \le \kappa \le 2$ , *i.e*,  $0 \le \delta \le 2\delta_o$ . Using *Cor.* 1 we can conclude that it is desirable to use old ranging measurements until the time elapsed since passing the waypoint is same as the time required to reach it initially, the PEB will be strictly lower by using the former set of measurements. Therefore the further the agent is from the waypoint, longer the aged measurements will be relevant.

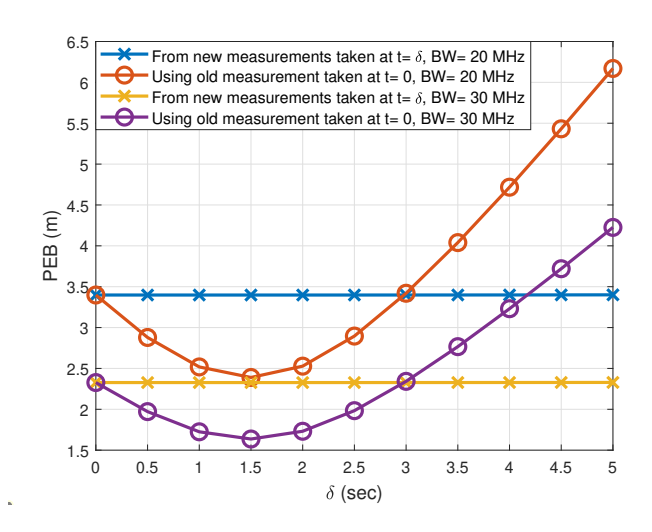


Fig. 4. PEB for estimating new position from aged measurements versus fresh measurements under a linear motion model. Parameters:  $v=3 \mathrm{ms}^-$ ,  $(x_t,y_t)=(4 \mathrm{m},8 \mathrm{m}), (x_o,y_o)=(0 \mathrm{m},10 \mathrm{m}).$ 

In Fig. 5, we compare the PEB of the future positions based on aged range measurements versus the PEB achieved by taking new measurements at that instant for the circular motion model. We observe that PEB decays with age, and it is always better to use fresh measurements. This is intuitively explained because initial uncertainty in location estimate contributes to additional uncertainty in turning radius and thus angular velocity calculation making our estimate go worse with time.

In Fig. 6, we compare the decay rate of PEB calculated as  $\frac{\text{PEB}[t_2]-\text{PEB}[t_1]}{t_2-t_1}$  against different values of turning radius. We observe that as the turning radius gets smaller, the PEB decays faster with age.

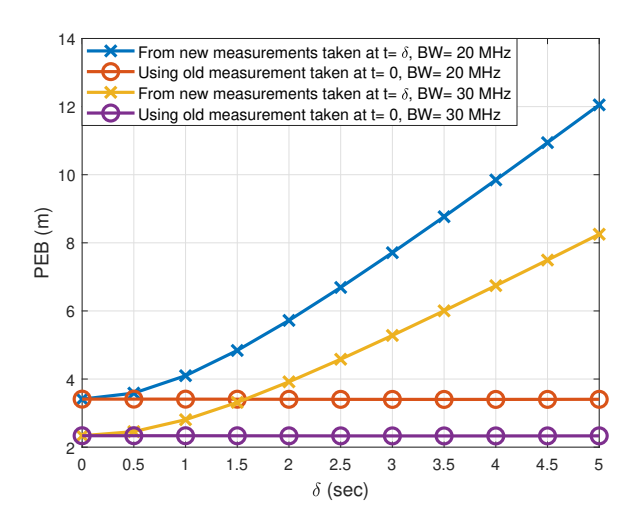


Fig. 5. PEB for estimating future positions from past measurements under circular trajectory model. Parameters:  $v=3\mathrm{ms}^-,~R=3\mathrm{m},~(x_c,y_c)=(10\mathrm{m},15\mathrm{m}),~\theta_o=30^o.$ 

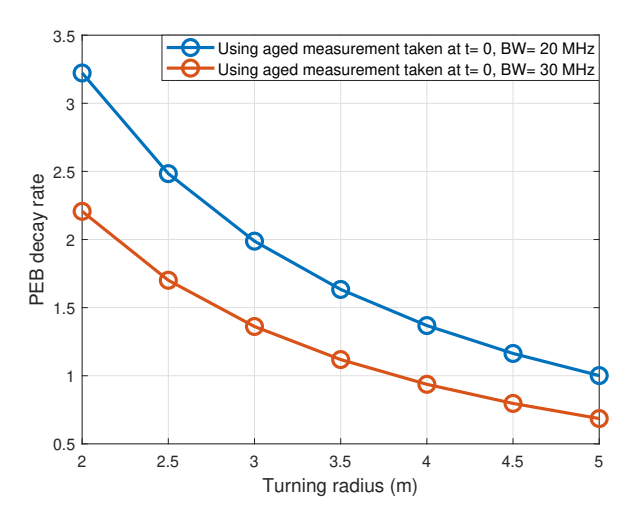


Fig. 6. Rate of change of PEB under circular trajectory model for different radius. Parameters:  $v=3 {\rm ms}^-$ ,  $(x_c,y_c)=(10 {\rm m},15 {\rm m})$ ,  $\theta_o=30^o$ ,  $t_1=1 {\rm s}$  and  $t_2=5$  s.

These observations yield key insights. Polling is required exactly once in traveling towards waypoints. As an extension of this, one can conclude that in traveling between multiple waypoints without involving turns, only one initial set of range measurements will be sufficient, and our estimate will get better with time. In between making a turn it is better to poll as frequently as possible. Further, we should place waypoints as far as possible from the obstacle corner so that the agent takes wider turns and the utility of aged data stays relevant for longer. Smaller turns make the location estimate go stale very quickly.

In Fig. 7, we plot the AoI curve showing the variation of PEB with time for the displayed trajectory in Fig. 3. Since polling operation involves getting visual cues as well, we

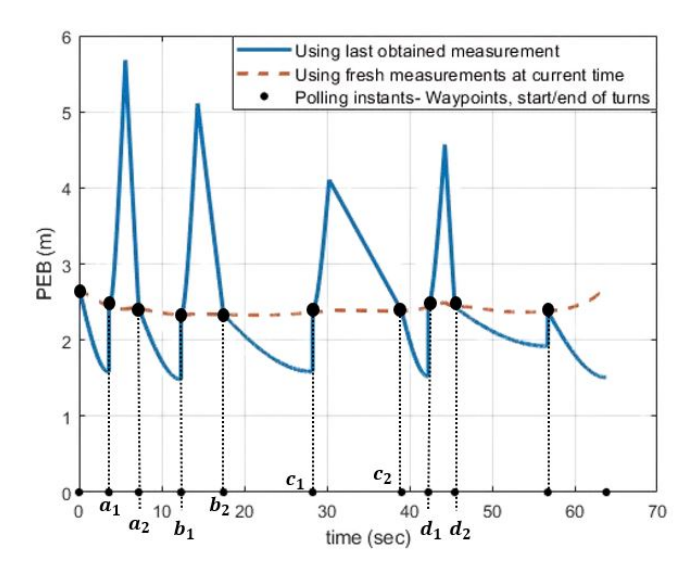


Fig. 7. PEB for the displayed trajectory in Fig. 3.  $a_1 \rightarrow a_2$ ,  $b_1 \rightarrow b_2$ ,  $c_1 \rightarrow c_2$  and  $d_1 \rightarrow d_2$  correspond to the time spent in turns. Parameters:  $v = 5 \text{ms}^-$ , BW = 30 MHz.

assume that new measurements are polled every time the agent is at a waypoint or is entering or leaving from a turn. However, from a perspective of solely position estimation, polling in between successive waypoints can also be skipped. In between the circular turns, we see that the PEB value rises well above the PEB achievable by taking a fresh measurement at that instant, the extent of jumps differ due to different turning radii.

In summary, the agent needs to poll when starting its motion, at the waypoints, and during the course of its circular turns.

#### V. CONCLUSION AND FUTURE WORK

Our analysis yields insights about the best performance an unbiased estimator can achieve for estimating future positions given old range measurements. Through a CRLB analysis we studied the effect an agent's motion has on the information content of aged range measurements. We were able to demonstrate that only one poll is sufficient to estimate future positions when an agent is following a rectilinear path guided towards a waypoint, further providing a better PEB than a fresh poll. For making turns modeled as circular arcs, we showed that it is better to poll as frequently as possible. We applied our analysis to a map-based navigation scenario and provided insights about the optimal frequency of polling and waypoint placement from the perspective of keeping aged measurements relevant for longer. Our results provide valuable insights toward selecting sensor polling instances for better battery utilization and spectrum usage in adversarial environments where frequent communication is limited or may not be established. Using our framework, it is possible to determine how often transmissions must occur in order to locate an uncooperative agent to within a certain accuracy. While CRLB analysis provide insights into the best performance an unbiased estimator can provide using a given set of observations, the design of such estimators is a different problem which is left as a future work. Integration of optimization techniques with our framework for resource allocation is an interesting extension to explore.

#### REFERENCES

- [1] Y. Shen and M. Z. Win, "Fundamental limits of wideband localization—Part I: A general framework," *IEEE Trans. on Info. Theory*, 2010.
- [2] K. Witrisal, P. Meissner, E. Leitinger, Y. Shen, C. Gustafson, F. Tufvesson, K. Haneda, D. Dardari, A. F. Molisch, A. Conti, and M. Z. Win, "High-Accuracy Localization for Assisted Living: 5G systems will turn multipath channels from foe to friend," *IEEE Sig. Proc. Mag.*, 2016.
- [3] H. K. Dureppagari, D.-R. Emenonye, H. S. Dhillon, and R. M. Buehrer, "Uav-aided indoor localization of emergency response personnel," in 2023 IEEE/ION Position, Location and Navigation Symposium (PLANS), 2023.
- [4] R. Zekavat and R. M. Buehrer, Handbook of position location: Theory, practice and advances. John Wiley & Sons, 2011, vol. 27.
- [5] S. Gezici, M. R. Gholami, S. Bayram, and M. Jansson, "Jamming of wireless localization systems," *IEEE Trans. on Commun.*, 2016.
- [6] J. Yan, Y. Meng, X. Luo, and X. Guan, "To hide private position information in localization for internet of underwater things," *IEEE Internet of Things Journal*, 2021.
- [7] M. Nain and N. Goyal, "Energy efficient localization through node mobility and propagation delay prediction in underwater wireless sensor network," Wirel. Pers. Commun., 2022.
- [8] N. Dutta, A. Saxena, and S. Chellappan, "Defending wireless sensor networks against adversarial localization," in 2010 eleventh Int. Conf. on mobile data management, 2010.
- [9] D. Mulvaney, Y. Wang, and I. Sillitoe, "Waypoint-based mobile robot navigation," in 2006 6th World Congress on Intelligent Control and Automation, 2006.
- [10] M. T. S. Ibrahim, S. V. Ragavan, and S. Ponnambalam, "Way point based deliberative path planner for navigation," in 2009 IEEE/ASME Int. Conf. on Adv. Intelligent Mechatronics. IEEE, 2009.
- [11] Y. Yi and X. Hu, "Robot simultaneous localization and mapping based on self-detected waypoint," *Cybernetics and Information Technologies*, 2016.
- [12] N. Pandey, G. Duggal, and S. S. Ram, "Database of simulated inverse synthetic aperture radar images for short range automotive radar," in 2020 IEEE Int. Radar Conf. (RADAR), 2020.
- [13] I. Ullah, Y. Shen, X. Su, C. Esposito, and C. Choi, "A Localization Based on Unscented Kalman Filter and Particle Filter Localization Algorithms," *IEEE Access*, 2020.
- [14] A. Eman and H. Ramdane, "Mobile robot localization using extended kalman filter," in 2020 3rd Intl. Conf. on Comp. Apps. & Info. Security (ICCAIS), 2020.
- [15] R. D. Yates, Y. Sun, D. R. Brown, S. K. Kaul, E. Modiano, and S. Ulukus, "Age of Information: An Introduction and Survey," *IEEE Journ. on Sel. Areas in Commun.*, 2021.
- [16] P. D. Mankar, Z. Chen, M. A. Abd-Elmagid, N. Pappas, and H. S. Dhillon, "Throughput and Age of Information in a Cellular-Based IoT Network," *IEEE Trans. on Wirel. Commun.*, 2021.
- [17] W. J. Hussain, A. K. Gupta, K. Pandey, and H. S. Dhillon, "Performance of mobile cyber-physical agents with discrete trajectories for sensing spatio-temporal variables," in 2023 57th Asilomar Conf. on Sig., Sys., and Comp., 2023.
- [18] S. M. Kay, Fundamentals of statistical signal processing: estimation theory. Prentice-Hall, Inc., 1993.
- [19] J. Wolf, W. Burgard, and H. Burkhardt, "Robust vision-based localization by combining an image-retrieval system with Monte Carlo localization," *IEEE Trans. on Robotics*, 2005.
- [20] A. Morar, A. Moldoveanu, I. Mocanu, F. Moldoveanu, I. E. Radoi, V. Asavei, A. Gradinaru, and A. Butean, "A comprehensive survey of indoor localization methods based on computer vision," *Sensors*, 2020.
- [21] N. J. Higham and S. H. Cheng, "Modifying the inertia of matrices arising in optimization," *Linear Algebra and its Applications*, 1998.